Available online at www.sciencedirect.com
SCIENCE DIRECT
Catalysis Today 100 (2005) 249–254
CATALYSIS TODAY
www.elsevier.com/locate/cattod

Relating catalyst structure and composition to the water–gas shift activity of Cu–Zn-based mixed-oxide catalysts

Magnus Rønning[a,*], Florian Huber[a], Hilde Meland[a], Hilde Venvik[b], De Chen[a], Anders Holmen[a]

[a]*Norwegian University of Science and Technology (NTNU), Department of Chemical Engineering, N-7491 Trondheim, Norway*
[b]*SINTEF Materials and Chemistry, N-7465 Trondheim, Norway*

Available online 28 December 2004

Abstract

In order to investigate the effect of cerium oxide on Cu–Zn-based mixed-oxide catalysts four catalyst samples were characterized by means of XRD, in situ XANES and thermogravimetric analysis. The activity of the catalyst samples was tested for the forward water–gas shift reaction. Cerium oxide was found to increase the crystallinity of the ZnO phase indicating a segregation of the Cu and ZnO phases. The TOF of the water–gas shift reaction based on chemisorption data was found to be independent of composition and preparation conditions of the four catalyst samples. In contrast, the catalyst stability depends on composition and preparation conditions. Cerium oxide impregnated before calcination of the hydrotalcite-based Cu–Zn precursors leads to a more stable water–gas shift catalyst.

Keywords: Water–gas shift; Copper; Cerium oxide; XANES; XRD; Thermogravimetric analysis

1. Introduction

The water–gas shift (WGS) reaction ($CO + H_2O \leftrightarrow CO_2 + H_2$) is an important step in the production of H_2 from hydrocarbons. Recently, the WGS reaction has received renewed interest as a key step in fuel processing to reduce the CO level in hydrogen produced for proton exchange membrane fuel cell (PEMFC) applications [1]. For low temperature WGS, Cu is usually preferred as the active component because of its proven activity [2,3]. However, there is a need for catalysts with even higher activity and stability compared to the traditional $CuO–ZnO–Al_2O_3$ system.

It has been shown that oxides with high oxygen storage capacity such as CeO_2 can exhibit high WGS activity in conjunction with various metal promoters [4–7]. The role of ceria in such systems is proposed to be via a ceria-mediated redox process where the oxygen storage capacity of ceria and the metal are the active elements [4,5,8]. Others have found evidence of a mechanism involving the reaction between CO and active OH groups to form surface formates [7,9–11]. The promoting metal in the form of e.g. Pt, Au or Cu significantly increases the WGS activity of ceria and enhances the reducibility of ceria [4,6]. In the presence of Cu, ceria reduction is proposed to start at low temperatures (<200 °C) [4]. Ceria is also believed to enhance reducibility and stabilise the Cu particles towards sintering [12]. For both cases, ceria as an active component and as a promoter, the results indicate that ceria is partially reduced in the active catalyst, most likely by surface reduction. However, the effect of ceria on the Cu metal particles is not clear.

In this study, we examine the effect of ceria addition on the Cu metal particles in $Cu–ZnO–Al_2O_3$ catalysts derived from layered hydroxide materials of the hydrotalcite structure [13]. Mixed-oxide catalysts derived from hydrotalcite-like materials are shown to possess high activity and thermal stability together with relatively high metal dispersion and homogeneous distribution of the components [14]. WGS activity measurements and deactivation studies are examined together with structural information from XRD, XANES and other techniques. However, reaction mechanisms are not being considered in this report. Kinetic considerations of the activity measurements will be treated elsewhere [15].

* Corresponding author. Tel.: +47 73594121; fax: +47 73595047.
E-mail address: ronning@chemeng.ntnu.no (M. Rønning).

0920-5861/$ – see front matter © 2004 Elsevier B.V. All rights reserved.
doi:10.1016/j.cattod.2004.09.059

2. Experimental

A series of Cu- and Zn-based catalysts derived from hydrotalcite structures were synthesised by co-precipitation of the precursor salts followed by subsequent aging, filtration, washing, drying and calcination. The aqueous anionic solution was made by dissolving Na_2CO_3 and NaOH. Nitrates of Cu, Zn and Al were added at 80 °C under continuous stirring and pH adjustment. The solution was aged for 15 h before being filtered and washed and dried in vacuum. The catalysts were impregnated with $Ce(NO_3)_3$ either before or after calcination. The sample labels (see Table 1) are related to the preparation conditions: Cu-350 means a $CuO–ZnO–Al_2O_3$ catalyst that was calcined for 6 h at 350 °C. A portion of this sample was impregnated with cerium nitrate after calcination before undergoing a second calcination for 6 h at 250 °C, resulting in the sample Ce-aC-350. Cu-400 is $CuO–ZnO–Al_2O_3$ with the same nominal composition as Cu-350 calcined for 6 h at 400 °C. Ce-bC-400 is based on Cu-400, but was impregnated with cerium nitrate before calcination for 6 h at 400 °C. Ce-aC-350 and Ce-bC-400 have the same nominal composition.

Copper dispersion measurements by means of selective oxidation via N_2O surface titration [16] were performed in a Thermogravimetric Analyser (Perkin Elmer TGA 7) using 10 vol.% N_2O in Argon (temperature: 75 °C, flow rate 80 ml/min at ambient temperature). Temperature-programmed reduction (TPR) using 7 vol.% H_2 or CO in Argon (heating rate: 2 K/min, flow rate: 80 ml/min at ambient temperature), as well as the estimation of the weight loss of the calcined samples assigned to adsorbed water and/or surface carbonates [6] was carried out in the same apparatus. The weight loss (at 260 °C for 1 h in Ar) was determined prior to reduction (at 260 °C for 2 h in 7 vol.% H_2 in Ar) and dispersion measurements. Dispersion calculations based on oxygen chemisorption from N_2O-decomposition of the reduced catalyst samples were corrected for bulk oxidation of copper according to a method proposed by Sato et al. [17].

XRD spectra for crystallite size estimation and phase identification were recorded on Siemens diffractometers D-5000 (monochromatic radiation) and D-5005 (dichromatic radiation), respectively. Particle size estimates for the reduced samples were calculated from experimental line broadening (linewidth at half maximum) of the Cu(1 1 1) reflection by using the Scherrer equation and LaB_6 as a standard for correction of instrumental line broadening. To do this, the catalysts were dried (at 260 °C for 1 h in Ar), reduced (at 260 °C for 2 h in 7 vol.% H_2 in Ar) and passivated (at ambient temperature for 2 h in 0.5 vol.% O_2 in Ar) in the TGA before transportation to the X-ray diffractometer. The crystallite sizes reported in Table 1 are corrected for the thickness of the passivation layer assuming a cubic model for the copper particles [18].

Transmission X-ray absorption spectroscopy (XAS) data were collected at the Swiss–Norwegian Beam Lines (SNBL) at the European Synchrotron Radiation Facility (ESRF), France. Spectra were obtained at the Cu K-edge (8.979 keV) and Zn K-edge (9.659 keV) using a channel-cut Si(1 1 1) monochromator. Ce K-edge data (40.444 keV) were recorded using a Si(3 1 1) monochromator. For the Si(1 1 1) monochromator higher order harmonics were rejected by means of a chromium-coated mirror aligned with respect to the beam to give a cut-off energy of approximately 15 keV. The beam currents ranged from 130 to 200 mA at 6.0 GeV. The maximum resolution ($\Delta E/E$) of the Si(1 1 1) bandpass is 1.4×10^{-4} using a beam of size 0.6 mm × 7.2 mm. Ion chamber detectors with their gases at ambient temperature and pressure were used for measuring the intensities of the incident (I_0) and transmitted (I_t) X-rays.

The XANES (X-ray absorption near edge structure) measurements were performed on two of the four catalysts, Cu-400 and Ce-bC-400. The amounts of material in the samples were calculated to give an absorber optical

Table 1
Chemical composition and physical properties for the catalyst samples

Sample	ICP-AES[a] catalyst composition mass fraction[b]					BET[c] (m^2/g)	H_2O/CO_2 loss[d] (%)	Cu dispersion[e] (%)	XRD[f]	
	Cu	Zn	Al	Ce	O				Cu crystal size (nm)	Dispersion (%)
Cu-350	0.29	0.39	0.08	0.00	0.24	72.4	5.7	6.5	23	3.8
Ce-aC-350	0.26	0.35	0.08	0.07	0.24	–	3.2	4.8	16	5.6
Cu-400	0.27	0.40	0.09	0.00	0.24	76.2	1.7	5.4	25	3.5
Ce-bC-400	0.25	0.37	0.08	0.06	0.24	–	1.7	8.2	23	3.8

[a] ICP-AES: inductively coupled plasma-atomic emission spectroscopy with an estimated detection limit of 0.01–0.03 mg/g. The elementary analysis was performed on calcined samples.

[b] Normalised mass fractions, i.e. only CuO, ZnO, Al_2O_3 and CeO_2 taken into account.

[c] Performed on the calcined samples, prior to reduction.

[d] Thermogravimetric measurements performed in Ar on the calcined samples up to the reduction temperature (260 °C) resulted in a weight loss assigned to adsorbed water and/or surface carbonates [6].

[e] Dispersion based on oxygen chemisorption (from N_2O) of the reduced catalyst samples taking into account copper bulk oxidation [17].

[f] Performed on the reduced and passivated samples. The copper crystallite size is estimated using the Scherrer equation for the Cu(1 1 1) reflection taking into account the thickness of the passivation layer. The copper dispersion is calculated from the crystallite size assuming a cubic particle shape with one face in contact with the support [18].

thickness close to 2 absorption lengths. The samples were ground and mixed with the requisite amount of boron nitride to achieve the desired absorber thickness. The samples were then loaded into an in situ reactor-cell [19] and reduced in a mixture of 5 vol.% H_2 or CO in He (purity: 99.995%; flow rate 30 ml/min at ambient temperature) by heating at a rate of 6 K/min from room temperature to 350 °C. XANES profiles were collected during heating of the samples to follow the reduction progression of CuO in H_2 or CO. Cu and Zn metal foils, Cu_2O, CuO and ZnO were used as reference materials.

The software package WINXAS v3.0 [20] was used for XANES analysis to obtain qualitative and quantitative information on copper, zinc oxide and cerium oxide bulk phases under temperature programmed reduction conditions. The XANES data were energy calibrated, pre-edge background subtracted (linear fit) and normalised. Principal component analysis (PCA) was applied for identification of the number and type of phases in the experimental XANES spectra. The reference spectra of these phases were then used in a least-square fitting procedure to determine the fraction of each phase present [21].

The initial water–gas shift activity was tested in an externally heated tubular fixed-bed reactor with on-line GC analysis over a wide temperature range (200–300 °C) [15]. In order to minimize temperature gradients the catalyst samples were diluted with inert SiC (300–600 μm) taking into account the falsifying effect of dilution on the measured catalyst conversion [22]. Parameters like catalyst amount, particle size, feed composition and gas flow rate were chosen to perform the activity measurements within the kinetic regime and away from the thermodynamic equilibrium of the water–gas shift reaction [23]. The catalysts (0.15–0.25 mg, 200–400 μm) were pre-reduced in situ at 260 °C for 3 h in 7 vol.% H_2 in nitrogen, and the activity tests were performed at a total pressure of 3 bar and 1.3 nl/min total flow (0.7 nl/min N_2, 0.3 nl/min CO, 0.3 nl/min H_2O). The deactivation measurements (feed: 1.0 nl/min N_2, 0.3 nl/min CO, 0.3 nl/min H_2O) were performed at 300 °C in order to accelerate the copper sintering process.

3. Results and discussion

The chemical composition and some physical properties of the catalyst samples are presented in Table 1. Phase identification was performed by XRD both before and after calcination. The nominal catalyst loadings were confirmed by inductively coupled plasma (ICP-AES). The copper content was also confirmed by the TPR-TGA analysis except for Ce-aC-350. For this catalyst, the extent of reduction exceeded the maximum copper equivalent indicating a reduction of components other than copper oxide. This effect is object for more studies and will not be discussed here in further detail.

XRD results confirm that the layered hydrotalcite phase was obtained and that it breaks down during calcination to produce mixed oxides (see Fig. 1(a)). The diffraction peaks associated with ZnO are significantly more intense in the samples containing ceria, for the calcined (Fig. 1(a)) as well as the reduced–passivated samples (Fig. 1(b)). This can be due to low crystallinity of ZnO in absence of ceria or simply arising from smaller ZnO crystallites. The enhanced ZnO crystallinity in the samples containing CeO_2 may indicate less interaction between ZnO and Cu in these samples. The shape of the main diffraction peak for CeO_2 at around 29° indicates either low CeO_2 crystallinity or small crystallites. It has been stated in the literature that ZnO is not an active reaction site in the water–gas shift reaction [2,3]. The XRD data suggest that addition of CeO_2 to the copper–zinc system induces segregation of Cu and Zn phases, whereas CeO_2 seems to be well dispersed. The Cu crystallite sizes are calculated from XRD line broadening analysis (XLBA) using the Scherrer equation and indicate particle sizes around 20 nm for the Cu(1 1 1) reflection (see Table 1).

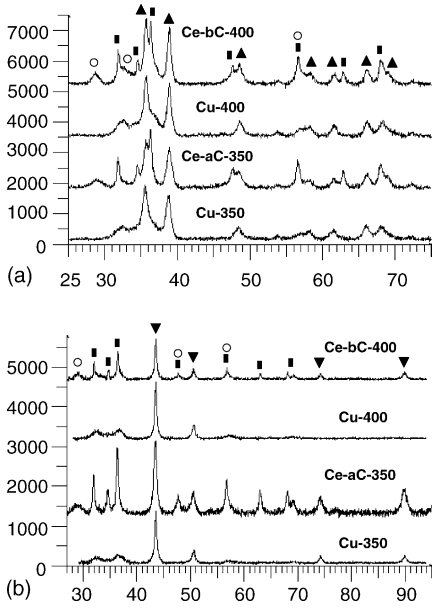

Fig. 1. XRD spectra of the (a) calcined and (b) reduced–passivated samples. The spectra of the calcined samples were recorded with D-5005. The reduced samples were recorded with D-5000 except the shown spectra for Ce-aC-350 which was also recorded with D-5005. The symbols on top of the spectra are related to the different phases: (■) ZnO, (▲) CuO, (▼) Cu, (○) CeO_2.

The Cu dispersion obtained from oxygen chemisorption show Cu dispersions of 4–8% (see Table 1). The sample impregnated with Ce before calcination shows highest dispersion (8%) whereas the Ce impregnation after calcination gives lower Cu surface area. These data are in good agreement with the dispersions calculated from XRD data (3.5–5.5%) in terms of the order of magnitude of copper dispersion in the catalyst samples. However, the dispersions derived from XLBA show a different trend. For turnover frequency (TOF) calculations, data from oxygen chemisorption have been used since this method gives a more direct, and thus presumably more accurate, estimate of the active

surface than the XLBA results from the reduced–passivated samples. The XLBA method is a bulk technique and derives the copper surface area indirectly from the crystallite size. The XLBA-derived dispersions depend on a structural model used for converting crystallite size into dispersion and taking into account the passivation layer (here: cubic model) and might therefore be a less realistic measure of the copper surface area. The estimates are useful, however, for validating the range of the chemisorption-based dispersions.

Currently, selective oxygen chemisorption via the decomposition of N_2O on the Cu surface is a widely used technique for measuring metallic Cu surface area of copper-based catalysts [16,17]. Nevertheless, uncertainties remain concerning N_2O decomposition on ceria and whether or not partially reduced cerium oxide corrupts the measured dispersion [3,18]. It still remains a matter of discussion whether chemisorption can be applied, or if this standard procedure needs some corrections.

In situ XANES measurements of the reduction behaviour of the catalysts at the Cu K-edge show that the bulk copper in the catalyst is reduced to the metallic state (see Fig. 2(a)). The reduction proceeds more easily in CO than in H_2 (results not shown here), since CO has a higher reduction potential than H_2 [24,25]. The transition goes directly from CuO to Cu, and Cu_2O is not detected (see Fig. 2(b)) at the given time resolution of the recorded XANES spectra. This is in agreement with recent studies [26] and suggests that Cu_2O is not a stable component under the applied reduction conditions. Agreement also exists between the XANES (Fig. 2(b)) and the TGA results (Fig. 3) concerning the transition temperature. Slight differences arise from the limited time resolution in the XANES experiments. Furthermore, the TGA experiments where carried out using a slightly higher H_2 concentration than the XANES experiments. According to Fig. 3, the catalyst Ce-aC-350 shows a notably higher reduction temperature than the other catalysts. A reason for this might be that copper is partially covered by cerium oxide. This effect will be addressed in further studies. Ceria does not enhance the reducibility of copper in any of the investigated catalysts. This is most likely because the co-operational effect of Cu and ceria in the WGS reaction is not present when ceria is in a state of low oxygen storage capacity [5].

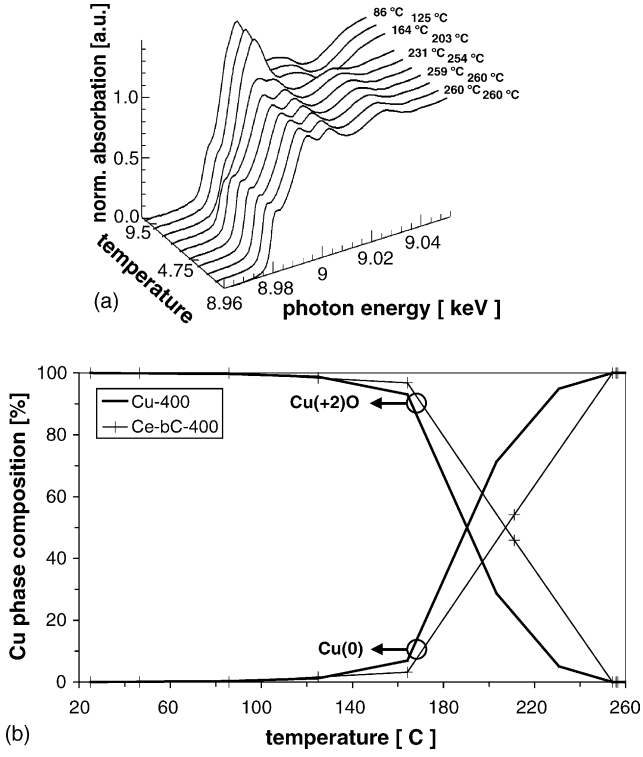

Fig. 2. TPR-XANES of Cu-400 at the Cu K-edge in 5 vol.% H_2 in helium. Heating rate: 6 K/min, flow rate: 30 ml/min at ambient temperature. (a) Cu K-edge profiles recorded during the reduction procedure. (b) Change in phase composition as a function of temperature during the reduction procedure showing the direct transition from CuO to Cu metal. Cu_2O was not detected during the transition process.

The effect of catalysts composition on the metal particles and the role of Ce will be more closely investigated by the proceeding EXAFS analysis [15]. However, both XRD and the EXAFS analysis support the conclusion drawn by Grunwaldt et al. [24], stating that the Cu metal particles take a disk-like shape under reducing conditions. This is reflected in a pronounced anisotropy in particle shape seen when analysing the particle size in different crystallographic directions [15].

Zn and Ce K-edge XANES profiles (not presented here) show that the bulk of ZnO and CeO_2 is not reduced under the applied conditions up to 350 °C, neither in H_2 nor in CO atmosphere. Since XANES is a bulk technique, surface oxidation of ZnO or CeO_2 is not detected but cannot be excluded.

The initial WGS activity of the four catalysts is shown in Fig. 4(a). The selectivity of the reaction was 100% towards CO_2 formation. The chemisorption-based turnover frequencies (TOFs) of the different catalysts are similar within the experimental accuracy, indicating that the WGS reaction depends on the exposed Cu surface area only [2,3]. Ceria seems to enhance copper dispersion (N_2O-based dispersion, Table 1) and catalyst stability (see Fig. 4(b)) when introduced before calcination. This indicates a promoting effect of ceria on the active copper sites and implies sufficient contact between both phases. The XRD spectra of the reduced–passivated catalysts (Fig. 2(b)) with broad ceria peaks with low intensity leads to the conclusion of ceria being present in the form of small crystallites, a prerequisite for a sufficient interface between copper and ceria. Ceria included after calcination seems to reduce the chemisorption-based Cu surface area and slightly increase the catalyst stability. Assuming coverage of Cu by ceria, a reduced amount of accessible copper surface atoms would result in a lower catalytic activity of Ce-aC-350 in terms of CO reaction rate normalised with metallic copper. Since the chemisorption-based TOF is similar to the other samples (Fig. 4(a)), the nature of the active site seems to be unchanged. This also supports the idea of ceria partially

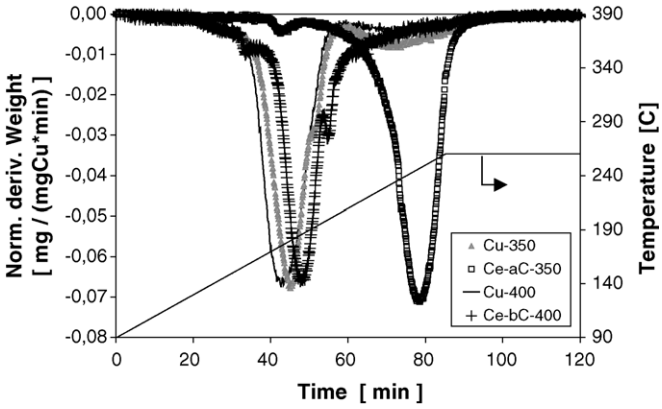

Fig. 3. Temperature-programmed reduction with 7% H_2 in Argon using a thermogravimetric device. Heating rate: 2 K/min, flow rate: 80 ml/min at ambient temperature. The weight derivative of the four catalyst samples normalised with the total weight loss during the reduction procedure and the temperature profile are plotted as a function of time.

covering the copper surface. Thus, diffusion limitations as a result of ceria coverage may explain the higher reduction temperature of Cu observed in the TPR profile of Ce-aC-350 (Fig. 3).

It is evident that the preparation procedure for introducing CeO_2 is important for the effect of CeO_2. As mentioned above, uncertainties still exist concerning the contribution of ceria to the measured dispersion based on oxygen chemisorption by means of N_2O surface titration. Comparing the N_2O-based dispersions of Cu-350 and Cu-400 also reveals a slight effect of the calcination temperature on the copper dispersion.

Sintering of the copper particles at elevated temperature close to the Huettig temperature (325 °C for copper), where

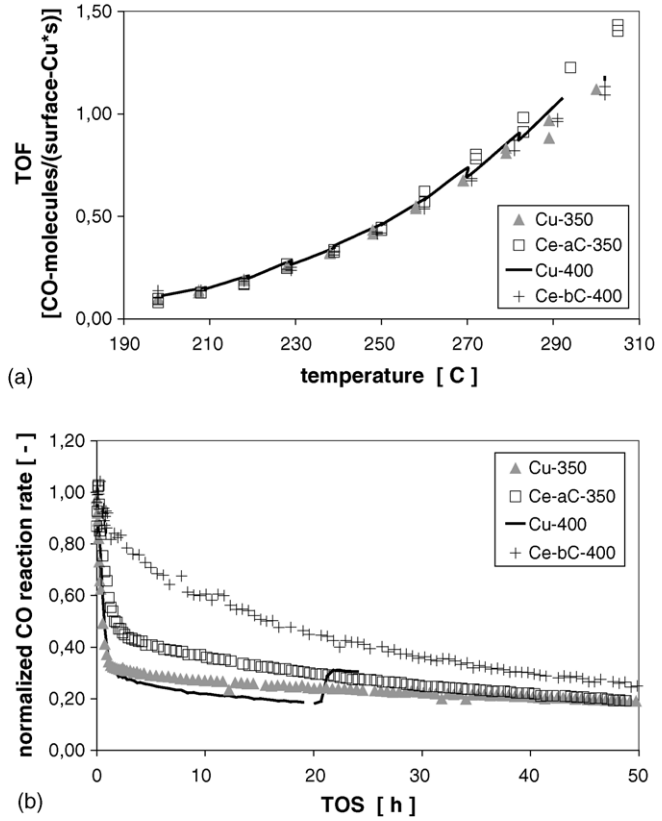

Fig. 4. (a) Turnover frequency (TOF) and (b) short-term deactivation behaviour of the catalyst samples. TOF is calculated from oxygen chemisorption (from N_2O) and corrected for loss of H_2O/CO_2. The deactivation measurements are performed at 300 °C and are presented as normalised reaction rates for the disappearance of CO vs. time on stream (TOS). The normalised reaction rates are not corrected for the H_2O/CO_2 uptake of the calcined samples, but as the corresponding catalysts exhibit a quite similar weight loss, this effect is negligible. The step in the deactivation curve for Cu-400 after 20 h stems from running out of nitrogen. This has no further effect on the deactivation behaviour of the catalyst.

copper atoms become mobile, is known to be a severe reason for catalyst deactivation under reaction conditions [27]. Steam enhances the sintering process. Experiments not shown here, however, indicate that the slight variations concerning the water vapour pressure between the four deactivation experiments have no visible influence on the deactivation behaviour.

4. Conclusions

A comparative study on the effect of cerium oxide on the water–gas shift activity of Cu–Zn-based mixed-oxide catalysts has been carried out using mainly XRD, in situ XANES and thermogravimetric analysis.

According to XRD data, the crystallinity of the ZnO phase increases when CeO_2 is included into the system. This might indicate a segregation of Cu- and Zn-containing phases resulting in a reduced interaction between Cu and ZnO. On the other hand, cerium oxide seems to be well dispersed. Activity measurements reveal that the chemisorption-based TOF of the investigated catalyst samples is independent of composition and preparation conditions. Together with the in situ XANES results, this leads to the conclusion that metallic copper is the active component. In contrast, the stability of the catalyst samples under reaction conditions depends on composition and preparation conditions. Thus, the stability can be increased by adding cerium oxide. In order to achieve this effect CeO_2 should be added before calcination of the hydrotalcite-based precursor.

Acknowledgements

This work was supported by the Research Council of Norway. We gratefully acknowledge the project team at the Swiss–Norwegian Beam Lines (SNBL) at the ESRF for their assistance. Elin Nilsen (Department of Materials Technology, NTNU) and Egil Haanæs (Department of Chemical Engineering, NTNU) are gratefully acknowledged for their assistance with XRD and TGA, respectively.

References

[1] Fuel Cell Handbook, 5th ed., US Department of Energy, NETL, 2000.
[2] C.V. Ovesen, B.S. Clausen, B.S. Hammershøi, G. Steffensen, T. Askgaard, I. Chorkendorff, J.K. Nørskov, P.B. Rasmussen, P. Stoltze, P. Taylor, J. Catal. 158 (1996) 170.
[3] N.A. Koryabkina, A.A. Phatak, W.F. Ruettinger, R.J. Farrauto, F.H. Ribeiro, J. Catal. 217 (2003) 233.
[4] Y. Li, Q. Fu, M. Flytzani-Stephanopoulos, Appl. Catal. B 27 (2000) 179.
[5] Q. Fy, A. Weber, M. Flytzani-Stephanopoulos, Catal. Lett. 77 (1–3) (2001) 87.
[6] G. Jacobs, E. Chenu, P.M. Patterson, L. Williams, D. Sparks, G. Thomas, B.H. Davis, Appl. Catal. A 258 (2004) 203.
[7] S. Hilaire, X. Wang, T. Luo, R.J. Gorte, J. Wagner, Appl. Catal. A 258 (2004) 271.
[8] T. Bunluesin, R.J. Gorte, G.W. Graham, Appl. Catal. B 15 (1998) 107.
[9] T. Shido, Y. Iwasawa, J. Catal. 136 (1992) 493.
[10] T. Shido, Y. Iwasawa, J. Catal. 141 (1993) 70.
[11] G. Jacobs, A. Crawford, L. Williams, P.M. Patterson, B.H. Davis, Appl. Catal. A 267 (2004) 27–33.
[12] M. Fernández-García, E. Gómez Rebollo, A. Guerrero Ruiz, J.C. Conesa, J. Soria, J. Catal. 172 (1997) 146.
[13] F. Cavani, F. Trifirò, A. Vaccari, Catal. Today 11 (1991) 173.
[14] M.J.L. Ginés, N. Amadeo, M. Laborde, C.R. Apesteguía, Appl. Catal. A 131 (1995) 283.
[15] F. Huber, M. Ronning, H. Meland, H. Venvik, D. Chen, A. Holmen, in preparation.
[16] A. Dandekar, R.T.K. Baker, M.A. Vannice, J. Catal. 183 (1999) 131.
[17] S. Sato, R. Takahashi, T. Sodesawa, K. Yuma, Y. Obata, J. Catal. 196 (2000) 195.
[18] N. Pernicone, T. Fantinel, C. Baldan, P. Riello, F. Pinna, Appl. Catal. A 240 (2003) 199.
[19] F.W. Lytle, R.B. Greegor, E.C. Marques, D.R. Sandstrom, G.H. Via, J.H. Sinfelt, J. Catal. 95 (1985) 546.
[20] T. Ressler, J. Synch. Rad. 5 (1998) 118–122.
[21] T. Ressler, J. Wong, J. Roos, I.L. Smith, Environ. Sci. Technol. 34 (2000) 950.
[22] R.J. Berger, J. Pérez-Ramírez, F. Kapteijn, J.A. Moulijn, Chem. Eng. Sci. 57 (2002) 4921.
[23] F. Kapteijn, J.A. Moulijn, in: G. Ertl, H. Knözinger, J. Weitkamp (Eds.), Handbook of Heterogeneous Catalysis, VCH Verlagsgesellschaft mbH, 1997(Chapter 9).
[24] J.-D. Grunwaldt, A.M. Molenbroek, N.-Y. Topsøe, H. Topsøe, B.S. Clausen, J. Catal. 194 (2000) 452.
[25] H. Wilmer, O. Hinrichsen, Catal. Lett. 82 (2002) 117.
[26] J.A. Rodriguez, J.Y. Kim, J.C. Hanson, M. Perez, A.I. Frenkel, Catal. Lett. 85 (2003) 247.
[27] M.V. Twigg, M.S. Spencer, Appl. Catal. A 212 (2001) 161.